7th International Conference on Silicon Photovoltaics, SiliconPV 2017

PV module current gains due to structured backsheets

Malte R. Vogt[a],*, Hendrik Holst[a], Henning Schulte-Huxel[a], Susanne Blankemeyer[a], Robert Witteck[a], Patrice Bujard[b], Jan-Bernd Kues[c], Carsten Schinke[d], Karsten Bothe[a], Marc Köntges[a], and Rolf Brendel[a,d]

[a]Institute for Solar Energy Research Hamelin (ISFH), Am Ohrberg 1, 31860 Emmerthal, Germany
[b]BASF Schweiz AG, Klybeckstrasse 141, 4057 Basel, Switzerland
[c]BASF Coatings GmbH, D403, Glasuritstrasse 1, 48165 Muenster, Germany
[d]Dep. Solar Energy, Inst. Solid-State Physics, Leibniz Universität Hannover, Appelstr. 2, 30167 Hanover, Germany

Abstract

We evaluate the optical performance of PV modules with respect to an increase in short circuit current density. Our evaluation is based on the combination of ray tracing simulations and measurements on test modules with four types of backsheets: Two of them are structured, the third is white and diffusively reflecting and the fourth reflects no light. Under normal incidence, structured backsheets reflect incoming light at an angle that causes total internal reflection at the glass/air interface, which guides the light to the solar cell surface. Three different irradiance conditions are studied: a) standard testing conditions (STC) with light incident perpendicular to the module surface, b) variation in the angle of incidence and c) light source with mean annual distribution of angles of incidence. Using the measured refractive index data in ray tracing simulations we find a short circuit current density (J_{sc}) gain of up to 0.9 mA/cm² (2.3%) for monofacial cells and a structured backsheet, when compared to a white backsheet with diffuse reflection. For bifacial cells we calculate an even larger J_{sc} increase of 1.4 mA/cm² (3.6%). The J_{sc} increase is larger for bifacial cells, since some light is transmitted through the cells and thus more light interacts with the backsheet. Our optical loss analysis reveals the best performance in STC for edge-aligned Ag grooves. This structure reduces absorption losses from 1.8 mA/cm² to 0.3 mA/cm² and reflection losses from 0.7 mA/cm² to 0 mA/cm². This trend also holds under various angles of incidence as confirmed consistently by J_{sc} measurements and ray racing simulations. Simulations using an annual light source emitting a mean annual distribution of angles of incidence reveal grooves in both orientations edge alignment and east-west alignment achieve similar current gains of up to 1.5% for mono- and of 2.5% for bifacial cells compared to modules with white back sheets. This indicates that for modules with light guiding structures such as these backsheets optimization for STC differs from optimization for annul yield.

* Corresponding author. Tel.: +49-511-762-17253.
  E-mail address: m.vogt@isfh.de

1. Introduction

We aim at increasing PV module efficiency by implementing light guiding structures to harvest light hitting the inactive areas of PV modules. Commonly used diffusely reflecting white backsheets typically guide half of the light hitting inactive areas onto the cells [1]. In contrast, metal coated structures can guide nearly 75% of this light onto the cell thereby increasing module efficiencies and power output [2][3][4] under standard testing conditions (STC) by around 1%. We analyze PV modules with entire backsheets comprising of triangular shaped metallic groove structures for monofacial cells and for bifacial cells.

2. Ray tracing model

Figure 1 depicts the triangular cross-section that is the basis for the grooves of the backsheet structure investigated in this study. We investigate two different alignments of many of those metal groove structures for the use as backsheet reflector:

- The grooves being aligned parallel to the cells' edges in each cell gap (Fig. 1, left), which we call "edge-aligned".
- The same grooves oriented parallel to two edges and orthogonal the two others (Fig. 1, right), which we call "east-west-aligned", because the grooves are meant be aligned in east-west direction.
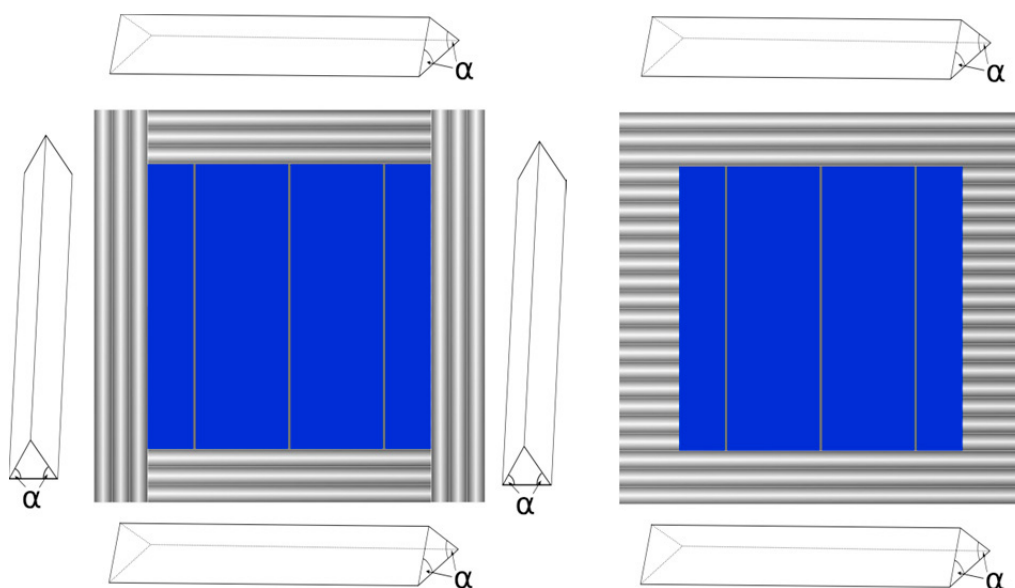

Fig. 1. Alignment of the structured backsheets with triangular grooves. Left: Grooves being aligned parallel to the four cell edges in each cell gap. Right the same grooves oriented parallel to the fingers, which we call "east-west-aligned".

We use the ray tracing framework DAIDALOS [5] to evaluate the optical performance of structured backsheets for PV modules. DAIDALOS models the glass cover, encapsulation, cell metallization and interconnects, cell texture, dielectric layers, local contacts as well as the various backsheet structures all as 3D geometries [6] with spectrally resolved optical constants.

Table 1 lists the geometrical features of the module and the optical constants of all materials (data are available

online in the references). All materials, except for the well known metals (Ag and Al), were optically characterized by ISFH. The standard cell interconnection ribbons (CIR), are modeled using the profile extracted from a cross sectional micrograph [7] with width 1.5 mm and height 232 μm. The fingers are modeled using the profile extracted from a scanning electron microscope (SEM) image [8] with a width of 60 μm and a height 18 μm. Please note that in this version of our simulation script the bifacial cells only have a rear texture, but no rear fingers and rear interconnectors are considered yet. The monofacial cells have a 154 mm × 154 mm rear metallization on a 156 mm × 156 mm wafer. The consequence is a 1 mm wide non-metallized cell region capable of collecting light incoming to the cells rear side. The solar front glass is a soda lime float glass with Fe_2O_3 weight total of 0.01‰ according to model 1 in Ref. [9]. The white backsheet with experimentally determined diffusive reflectivity [8] and a perfectly black backsheet with a reflectivity of zero serve as references for the structured backsheets whose surface is covered by either Ag or Al.

Table 1. Module components optical properties and thicknesses as used in experimental test modules and ray tracing simulations.

Module component	Material	Thickness
Glass	Low iron float glass [9]	4 mm
Encapsulant	EVA with enhanced UV transmission [10]	450 μm above cells
		200 μm between cells
		450 μm below cells
Connectors	Solder alloy coating (Sn62.5/Pb36/Ag1.5) [7]	232.4 μm
Fingers	Ag [11]	20 μm
Cell front ARC	$SiN_{n=1.9}$ [12]	72 nm
Cell	Si (n [12]; k [13])	180 μm
Cell rear side dielectric	$SiN_{n=2.13}$ [12]	200 nm
Cell full area rear metallization	Al [14]	20 μm
Backsheet	Varied	Varied

We model full square mono- and bifacial passivated emitter and rear solar cells (PERC) in a high efficiency module with an electrical power output of 300 W. In Ref. [4] we demonstrated that our simulation approach is capable of reproducing experimental measurement results with only 0.01 A deviation in I_{sc}.

3. Results at standard testing conditions

For standard test conditions (STC) we model a light source with rays orthogonally incident to the module glass surface and AM1.5G spectrum (IEC 60904-3, Ed. 2.0). The wavelength range is 300 to 1200 nm divided in 10 nm steps. We simulate 10 000 rays per wavelength at random positions. From the ray tracing results we calculate the photo generated current density J_{gen} (λ). This current density is related to the short circuit current density $J_{sc} = \int \eta(\lambda) J_{gen}(\lambda) \, d\lambda$ via the collection efficiency $\eta(\lambda)$. We model the semiconductor properties numerically using SENTAURUS [15] to derive the collection efficiency.

3.1. Ray tracing results for full-square monofacial cells

Figure 2 shows the optical loss analysis based on our ray tracing simulations of modules with monofacial solar cells. While the left part of Figure 2 shows the results for standard white backsheet and thus serves as a reference, the right part shows the loss analysis for a structured backsheet with edge-aligned Ag coated grooves. As can be seen from Figure 2, the optical performance of this module is improved in two ways:

- The structure of the backsheet reduces the amount of light that is reflected by the backsheet and escapes from the module through the front glass without ever hitting any part of cell. This reflection loss is reduced by 0.7 mA/cm² and can be seen as dark red part in Fig. 2.
- The higher reflectivity of the EVA-Ag interface compared to the EVA-backsheet interface reduces the amount of light absorbed by the backsheet. This absorption loss is reduced by 0.4 mA/cm² and can be seen as light green part in Fig. 2.
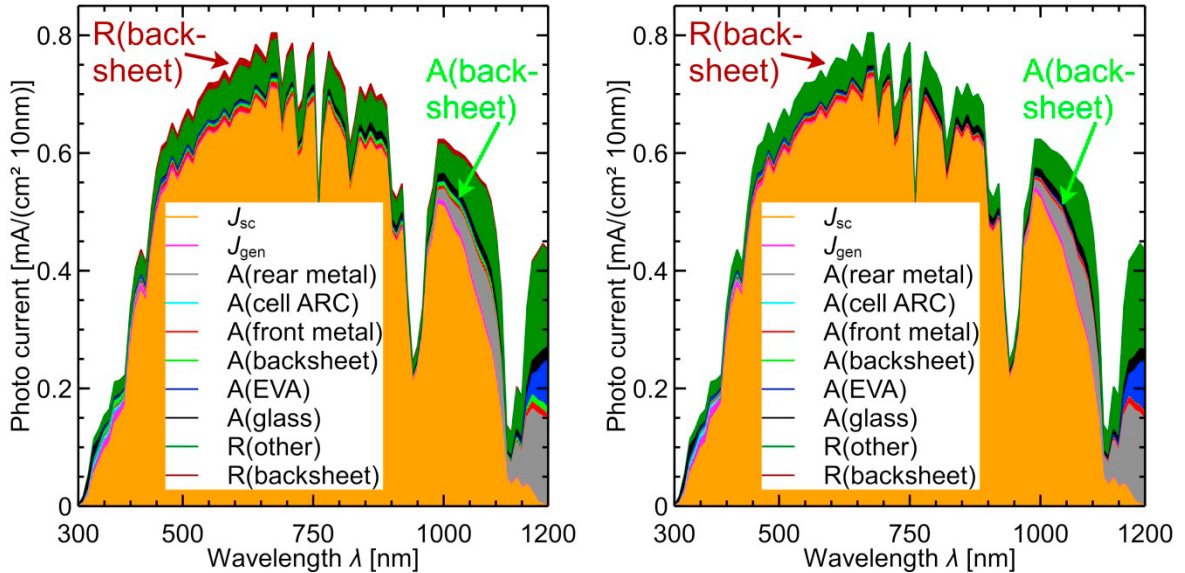

Fig. 2. Loss analysis of the PV modules with monofacial cells: Replacing the standard white backsheet (left) with the edge-aligned Ag coated grooves backsheet (right) reduces the reflection escaping the module (dark red) by 0.7 mA/cm² and the absorption in the backsheets (light green) by 0.4 mA/cm². Of these 1.1 mA/cm² in backsheet related loss reductions: 0.9 mA/cm² are converted into cell current gains, while the other 0.2 mA/cm² are turned into optical losses related to other module components. For cell gap width 4 mm.

In sum the backsheet related losses R(backsheet) and A(backsheet) are reduced by 1.1 mA/cm². Since the other module parts now interact with this additional light the other optical losses are increased by 0.2 mA/cm². The remaining 0.9 mA/cm² are converted into a short circuit current density (J_{sc}) gain of 2.3%.

Table 2 lists the J_{sc}-gains (integral over the orange part of Fig. 2) for various backsheets. Replacing the reference backsheet with aluminum coated grooves aligned parallel to the cells edges results in an increase in J_{sc} by 2.1%, while the east-west-aligned Al coated grooves decrease J_{sc} by 0.1% relative to the reference. Increasing the reflectivity (e.g. using Ag instead of Al) increases the current by 0.2% in case of monofacial cells.

Increasing the cell gaps, we find an increase in the J_{sc} gains (compared with the white backsheet) for edge-aligned aluminum grooves of up to 3.2% for 6 mm gaps. This increase follows from the capability of the aluminum coated grooves to guide light over several mm onto the cell.

The light recovery probability k of a backsheet[1] is a measure of the efficiency with which the light hitting the backsheet is redirected to the cells and converted into current. It is defined as

$$k_i = \frac{(I_{sc.i} - I_{sc.bbs}) \times A_{Cell}}{I_{sc.bbs} \times A_{BS}}, \tag{1}$$

where $I_{sc.i}$ is the short circuit current of the module with backsheet i, $I_{sc.bbs}$ is the short circuit current of the module with a black backsheet that reflects no light, A_{Cell} is the solar cell area and A_{BS} is the backsheet area around the cell reaching half the cell spacing wide[1]. The light recovery probability k is one if light hitting the backsheet is

guided to the cell and absorbed to contribute to the short circuit current with the same probability as if where hitting the cell directly and zero if no light hitting the backsheet is converted into short circuit current.

The light recovery probability of the different backsheet types are listed in the right column of table 2. All modules with a black backsheet, which reflects no light have a $k = 0$. The modules with white diffusely reflecting backsheet have a recovery probability between 0.51 for a 2 mm cell gap and 0.42 for 6 mm cell gap.

Table 2. J_{sc} for modules with full square monofacial PERC cells in modules with structured backsheets coated with aluminum or silver in different alignments under STC. The simulation uncertainty is ±0.05 mA/cm² and ±0.2%. The gain is calculated relative to a white backsheet.

Backsheet type	Cell gap [mm]	J_{sc} per cell area [mA/cm^2]	Gain [%]	Light recovery probability k
Black backsheet	2	37.97	-1.3	0
Reference: White backsheet	2	38.47	0.0	0.51
Edge-aligned Al grooves	2	38.8	0.9	0.88
Black backsheet	4	37.92	-2.4	0
Reference: White backsheet (Fig. 2)	4	38.83	0.0	0.46
Edge-aligned Al grooves	4	39.65	2.1	0.85
Edge-aligned Ag grooves (Fig. 2)	4	39.73	2.3	0.92
East-west-aligned Al grooves	4	38.79	-0.1	0.44
East-west-aligned Ag grooves	4	38.87	0.1	0.48
Black backsheet	6	37.97	-3.2	0
Reference: White backsheet	6	39.23	0.0	0.42
Edge-aligned Al grooves	6	40.48	3.2	0.84

For edge-aligned aluminum grooves our results show recovery probabilities between 0.88 and 0.84 decreasing with increased cell spacing. Replacing aluminum coating with silver coating increases the light recovery probability by 0.07.

For the east-west-aligned grooves the recovery probability lies between 0.48 for silver and 0.44 for aluminum. These results can be understood by looking at the alignment (see Fig. 1 right). For the two gaps, where the grooves are parallel to the cell edge, nearly all light is guided onto the cell. For the other two gaps, however, the grooves are orthogonal to the cell edge, thus the light is guided from one groove to another without ever hitting the cell. This behavior is true for light under normal incidence as is the case under STC in more realistic conditions this "east-west" alignment becomes more advantageous (see section 4).

3.2. Comparison with experimental test module

We fabricate an experimental test module with edge-aligned aluminum grooves in the 4 mm wide cell gaps as shown by the left part of Fig. 3. We use a AAA flasher to measure the I_{sc} for different angles of incidence. For more details see Ref. [1]. The measured I_{sc} values confirm the simulated angle dependence of the test module as shown on the right part of Fig. 3.
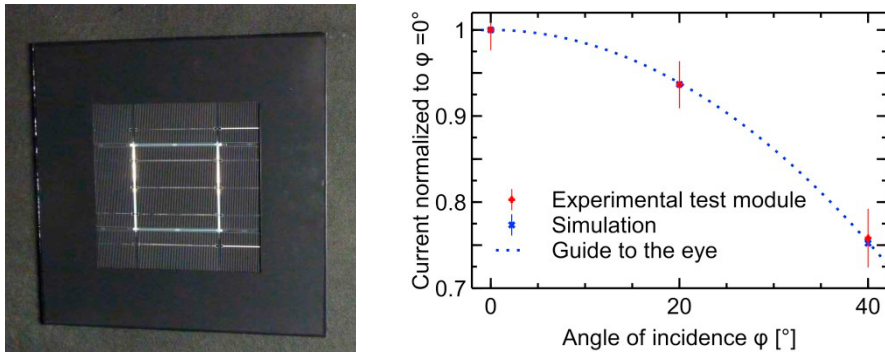
Fig. 3. Left: Experimental test module with edge-aligned grooves. Right: Comparison of simulation and experiment current dependency on angle of incidence after normalization to the value for 0°. The bar is the measurement uncertainty. The line is guide to the eye.

3.3. Ray tracing results for bifacial cells

Figure 4 shows the optical loss analysis based on our ray tracing simulations of modules with bifacial solar cells. While the left part of Figure 4 shows the results for standard white backsheet and thus serves as a reference, the right part shows the loss analysis for a structured backsheet with edge-aligned Ag grooves.

While the reference backsheet absorbs 1.8 mA/cm² (Fig. 4 left, light green), the structured backsheet absorbs 0.3 mA/cm² (Fig. 4 right, light green). If the metal was Al instead of Ag the absorption corresponded to a loss of 0.7 mA/cm².
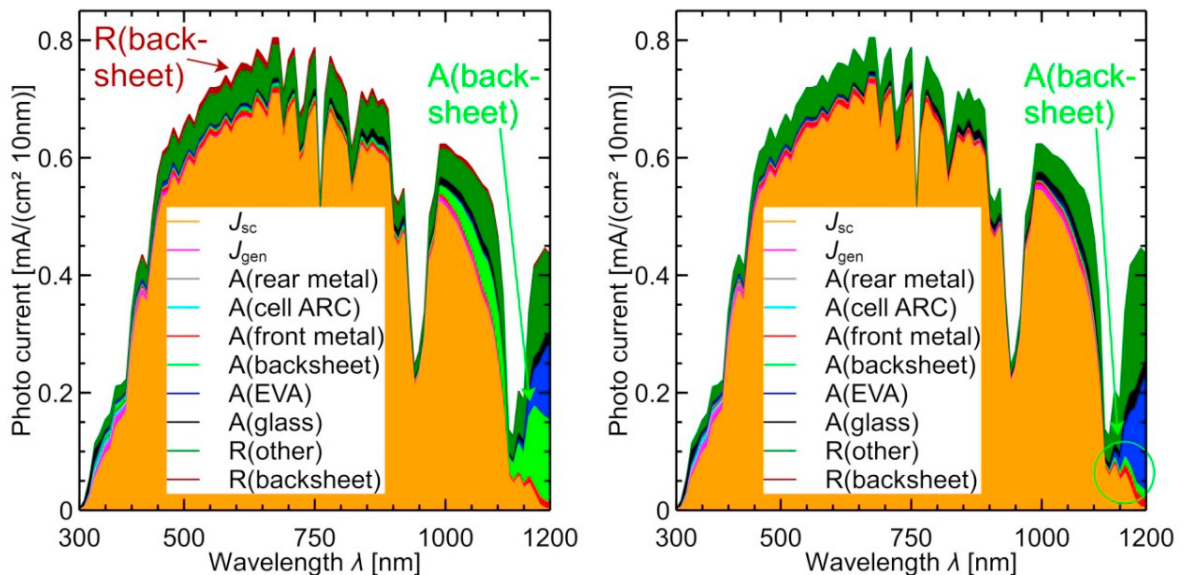

Fig. 4. Loss analysis of the PV modules with bifacial cells: Replacing the standard white backsheet (left) with a the edge-aligned Ag grooves backsheet (right) causes the absorption in the backsheets (light green) to be reduced by 1.5 mA/cm² and the reflection escaping the module (dark red) to be reduced by 0.7 mA/cm². Of these 2.2 mA/cm² in backsheet related loss reductions: 1.6 mA/cm² are converted into cell current gains, while the other 0.6 mA/cm² are turned into optical losses related to other module components. For cell gap width 4 mm.

We count light rays as reflected by the backsheet (dark red), if they leave the module through the glass, hit the backsheet at least once and never hit the cell. For a cell spacing area of 5% of the module area the reflection losses of the white backsheet R(backsheet) are 0.7 mA/cm² (left, dark red) whereas the edge-aligned grooves reduce the R(backsheet) loss to 0 (right, no dark red). This reduction in reflection losses is due to the grooves reflecting light to

the glass/air interface under angle causing total reflection back to the cells. The reduction of reflection losses R(backsheet) due to replacing the standard white backsheet with the structured backsheet is nearly the same for mono- and bifacial cells.

The higher reflectivity of the structured backsheets has a higher impact on bifacial cells since light rays can pass through the cells and exit at the rear side of the cells. Thus for the module with bifacial cells and reference white backsheet there is 1.8 mA/cm² absorption loss (Fig. 4 left, light green) mainly in the wavelength range 950-1200 nm, where the absorption coefficient of Si [13] is lower, but band to band absorption still occurs. In this wavelength range the avg. reflectivity is 0.75 for the white standard backsheet, 0.93 for Al and 0.97 for Ag (all reflectivities are at an interface with EVA). Consequently, our results for bifacial cells show higher current gains than for monofacial cell with the same backsheet.

Table 3 compares the current gains for monofacial and bifacial cells for different backsheets. PV modules with backsheets entirely covered with the metallized grooves structure show 0.9-1.3% higher current gains with the case of bifacial cells than in the case for monofacial cells due to the backsheet acting as the cells rear reflector. The highest current gain is 1.4 mA/cm² (3.6%) for edge-aligned Ag grooves, where only 0.3 mA/cm² is lost due to absorption in the backsheet (Fig. 4 right, light green).

Table 3. J_{sc} for bifacial cells in modules with various structured backsheets under STC. The simulation uncertainty is ±0.05 mA/cm² and ±0.2%. The gain is calculated relative to a white backsheet. For cell gap width 4 mm.

Backsheet type	Monofacial cell J_{sc} [mA/cm²]	Gain [%]	Bifacial cell J_{sc} [mA/cm²]	Gain [%]
Black backsheet	37.92	-2.4	37.19	-5.3
Reference: White backsheet	38.83	0.0	39.26	0.0
Edge-aligned Al grooves	39.65	2.1	40.46	3.1
Edge-aligned Ag grooves	39.73	2.3	40.68	3.6
East-west-aligned Al grooves	38.79	-0.1	39.56	0.8
East-west-aligned Ag grooves	38.87	0.1	39.79	1.3

4. Current gains under realistic irradiation

Realistic field irradiation conditions differ from STC in angle of incidence and spectral distribution. Hence, we utilize a yearly average light source to gain a realistic prediction of the improvement due to the structured backsheets. This light source emits a mean annual daylight distribution that models the celestial hemisphere by a partition into solid-angle intervals of 5° azimuth and 5° altitude. Each of these intervals contains its own spectral distribution and intensity [16]. For comparison, the overall intensity is normalized to 1000 W/m² in order to match the intensity of the AM1.5G spectrum.

The simulated modules are facing south with a 35° tilt angle, thus the east-west-aligned grooves are oriented in the east-west direction. The daily sun path is thus along the east-west-aligned grooves. This groove orientation also redirects most of the morning and evening sun rays to the cell. Consequently, the east-west-aligned grooves structure improves from 0% J_{sc} gain under normal incidence to 1.0%-1.5% J_{sc} gain under realistic irradiation. For all other tested structures the J_{sc} gains are lower than under STC due to optimization for normal incidence. Thus our results show that for modules with light guiding structures such as these backsheet optimization for STC differs from optimization for annul yield.

However, even under realistic irradiation our results show gains of up to 1.5% for mono- and up to 2.5% for bifacial cells with structured backsheets compare to module with a white backsheet as reference. Both orientations edge alignment and east-west alignment achieve similar current gains with the statistical one sigma simulation uncertainties (±0.2%) of the Monte-Carlo overlapping. This is important since backsheet with only east-west-aligned grooves is potentially easier to fabricate as well as independent of cell size and cell spacing than the edge-aligned grooves structure.

Table 4. J_{sc} for various structured backsheets with Al and Ag reflector under realistic irradiation. The simulation uncertainty is ±0.05 mA/cm² (±0.2%). The gain is calculated relative to a white backsheet. For cell gap width 4 mm.

Backsheet type	Monofacial cell J_{sc} [mA/cm²]	Gain [%]	Bifacial cell J_{sc} [mA/cm²]	Gain [%]
Black backsheet	37.52	-2.2	36.66	-5.2
Reference White backsheet	38.35	0.0	38.68	0.0
Edge-aligned Al grooves	38.60	0.7	39.36	1.7
Edge-aligned Ag grooves	38.83	1.3	39.63	2.5
East-west-aligned Al grooves	38.74	1.0	39.38	1.8
East-west-aligned Ag grooves	38.94	1.5	39.58	2.3

5. Conclusion

We evaluated the optical performance of PV modules with respect to an increase in short circuit current density. Our evaluation is based on the combination of ray tracing simulations and measurements on test modules with four types of backsheets: Two of them are structured, the third is white and diffusively reflecting and the fourth reflects no light. Under normal incidence, structured backsheets reflect incoming light at an angle that causes total internal reflection at the glass/air interface, which guides the light to the solar cell surface. Three different irradiance conditions were studied: a) standard testing conditions (STC) with light incident perpendicular to the module surface, b) variation in the angle of incidence and c) light source with mean annual distribution of angles of incidence.

Using the measured refractive index data in ray tracing simulations we find a short circuit current density (J_{sc}) gain of up to 0.9 mA/cm² (2.3%) for monofacial cells and a structured backsheet, when compared to a white backsheet with diffuse reflection. This trend also holds under various angles of incidence as confirmed consistently by J_{sc} measurements and ray racing simulations. For edge-aligned grooves the J_{sc} gain strongly depends on the width of the cell gap with 0.9% (for 2 mm), 2.1% (for 4 mm) to 3.2% (for 6 mm) in case of aluminum. Replacing aluminum with silver offers a current gain of 0.2% for the monofacial case.

For bifacial cells we calculate an even larger J_{sc} increase of 1.4 mA/cm² (3.6%). The J_{sc} increase is larger for bifacial cells, since some light is transmitted through the cells and thus more light interacts with the backsheet. PV modules with backsheets entirely covered with the metallized grooves structure show 0.9-1.3% higher current gains with the case of bifacial cells than in the case for monofacial cells due to the backsheet acting as the cells rear reflector. This demonstrates, that the reduction of backsheet absorption losses for monofacial modules fabricated with bifacial cells offers higher gains than for monofacial cells.

Our optical loss analysis reveals the best STC performance for edge-aligned Ag grooves. The reduction of backsheet reflection losses from 0.7 mA/cm² to 0 mA/cm² for the ideal structure is the same for bi- and monofacial cells. In contrast the absorption loss in the backsheet is reduced by 0.4 mA/cm² for mono- and 1.5 mA/cm² bifacial cells.

For the reference modules with the white standard backsheet our results are that the bifacial PERC cells achieve a 0.4 mA/cm² higher J_{sc} than the monofacial PERC cells. Our results for the structured backsheets show an up 0.9 mA/cm² higher J_{sc} for bi- compared to monofacial PERC cells. Thus our results suggest that its advantageous to use compared a monofacial PERC cell will increase, if no improvements of the monofacial PERC cells rear reflector are made.

Simulations using an annual light source emitting a mean annual distribution of angles of incidence reveal grooves in both orientations edge alignment and east-west alignment achieve similar current gains (within each others simulation uncertainty) of up to 1.5% for mono- and of 2.5% for bifacial cells compared to modules with white back sheets. This is in contrast to STC, where the east-west alignment results in 2.2-2.3% less current than the edge alignment for both cell types. Consequently, our results show that for modules with light guiding structures such as these backsheet optimization for STC differs from optimization for annul yield.

Acknowledgements

References

[1] Köntges M, Schulte-Huxel H, Blankemeyer S, Vogt MR, Holst H, Reineke-Koch R, Witteck R, Bothe K, Brendel R. Method to measure light recovery probablility of PV module backsheet enabling 20.2% module efficiency with PERC cells. 32nd EUPVSEC 2016;1532–8.

[2] Chung I, Lee WJ, Cho EC, Moon IS. Light Capturing Film for power gain of silicon PV modules. IEEE 40th PVSC 2014;2689–92.

[3] Zhang S, Deng W, Pan X, Jiao H, Chen D, Huang H, Cui Y, Xu J, Feng J, Zhong M, Chen Y, Altermatt PP, Feng Z, Verlinden PJ. 335Watt world record P-type mono-crystalline module with 20.6 % efficiency PERC solar cells. IEEE 42nd PVSC 2015;1–6.

[4] Schulte-Huxel H, Witteck R, Holst H, Vogt MR, Blankemeyer S, Hinken D, Dullweber T, Bothe K, Köntges M, Brendel R. High-Efficiency Modules With Passivated Emitter and Rear Solar Cells — An Analysis of Electrical and Optical Losses, IEEE JPV 2017;7(1):25–31.

[5] Holst H, Winter M, Vogt MR, Bothe K, Köntges M, Brendel R, Altermatt PP. Application of a new ray tracing framework to the analysis of extended regions in Si solar cell modules. Energy Procedia 2013;38:86–93.

[6] Winter M, Vogt MR, Holst H, Altermatt PP. Combining structures on different length scales in ray tracing: analysis of optical losses in solar cell modules. Opt. Quantum Electron 2015;47(6):1373–9.

[7] Holst H, Schulte-Huxel H, Winter M, Blankemeyer S, Witteck R, Vogt MR, Booz T, Distelrath F, Köntges M, Bothe K, Brendel R. Increased Light Harvesting by Structured Cell Interconnection Ribbons: An Optical Ray Tracing Study Using a Realistic Daylight Model. Energy Procedia 2016; 92:505–14.

[8] Witteck R, Schulte-Huxel H, Holst H, Hinken D, Vogt MR, Blankemeyer S, Köntges M, Bothe K, Brendel R. Optimizing the Solar Cell Front Side Metallization and the Cell Interconnection for High Module Power Output. Energy Procedia 2016; 92:531-9.

[9] Vogt MR, H. Hahn, Holst H, Winter M, Schinke C, M. Kontges, Brendel R, Altermatt PP. Measurement of the Optical Constants of Soda-Lime Glasses in Dependence of Iron Content and Modeling of Iron-Related Power Losses in Crystalline Si Solar Cell Modules. IEEE JPV 2016; 6(1):111–8.

[10] Vogt MR, Holst H, Schulte-Huxel H, Blankemeyer S, Hinken D, Witteck R, Winter M, Min B, Schinke C, Ahrens I, Köntges M, Bothe K, Brendel R. Optical constants of UV transparent EVA and the impact on the PV module output power under realistic irradiation. Energy Procedia 2016;92:523–30.

[11] Palik ED. Handbook of Optical Constants of Solids. Academic Press Inc., 1985.

[12] Vogt MR. Development of Physical Models for the Simulation of Optical Properties of Solar Cell Modules. Leibniz University Hannover, 2015.

[13] Schinke C, Christian Peest P, Schmidt J, Brendel R, Bothe K, Vogt MR, Kröger I, Winter S, Schirmacher A, Lim S, Nguyen HT, MacDonald D. Uncertainty analysis for the coefficient of band-to-band absorption of crystalline silicon. AIP Adv 2015;5(6): 67168.

[14] Shiles E, Sasaki T, Inokuti E, Smith DY. Self-consistency and sum-rule tests in the Kramers-Kronig analysis of optical data: Applications to aluminum. Phys. Rev. B 1980;22(4):1612–28.

[15] Synopsys Incorporation. Sentaurus Device. Mountain View, CA, USA.

[16] Winter M, Holst H, Vogt MR, Altermatt PP. Impact of realistic illumination on optical losses in Si solar cell modules compared to standard testing conditions. 31st EU PVSEC 2015;1869–74.